Ti-Cu-Zr-Fe-Sn-Si-Ag-Pd Bulk Metallic Glasses with Potential for Biomedical Applications

CHENHE WANG, NENGBIN HUA, ZHENLONG LIAO, WEI YANG, SHUJIE PANG, PETER K. LIAW, and TAO ZHANG

$Ti_{47}Cu_{38-x}Zr_{7.5}Fe_{2.5}Sn_2Si_1Ag_2Pd_x$ (x = 1, 2, 3, and 4 atomic percent, at. pct) bulk metallic glasses (BMGs) with potential for biomedical applications were fabricated by copper-mold casting. The Ti-based BMGs exhibited high glass-forming ability (GFA) with critical diameters of 4 to 5 mm and a supercooled liquid region over 50 K, though the high contents of Pd slightly decreased the GFA. The additions of 2 and 3 at. pct Pd benefited the improvement of plasticity, and the resultant BMGs showed the relatively low Young's modulus of about 100 GPa, high compressive strengths of 2174 to 2340 MPa, and compressive plastic strain of around 4 pct. The addition of Pd also decreased the passive current density and increased the pitting potential of the Ti-based BMGs in the Hank's solution, leading to the enhanced bio-corrosion resistance of the BMGs. Furthermore, the cell adhesion, viability, and proliferation behaviors revealed that the present Ti-based BMGs possess as good biocompatibility as that of the Ti-6Al-4V alloy. These results demonstrated the potential of the Ti-Cu-Zr-Fe-Sn-Si-Ag-Pd BMGs as biomedical materials.

https://doi.org/10.1007/s11661-021-06183-y

I. INTRODUCTION

OWING to the unique amorphous microstructure, Ti-based bulk metallic glasses (BMGs) exhibit relatively lower Young's moduli, higher strengths, and paralleled corrosion resistance in comparison with conventional biomedical crystalline titanium alloys.[1–7] For biomedical applications, these advantages of the Ti-based BMGs are favorable for relieving the "stress-shielding effect," improving the load-bearing capability, and maintaining the original mechanical properties of the implants during the long-term service under the aggressive human body environment.[1,4,6] Therefore, the Ti-based BMGs free from highly toxic elements, such as Be and Ni, have attracted attentions as potential metallic biomaterials.[2–5] Among them, the Ti-Zr-Cu-Pd(-Sn) system BMGs possess high glass-forming ability (GFA), suitable bio-mechanical properties, and good biocompatibility, whereas the contents of the noble element, Pd, with the high cost in the BMGs are relatively large.[4,8] Recently, we have found that the Ti-Cu-Zr-Fe-Sn-Si-(Ag, Sc) BMGs free from highly toxic elements exhibited good mechanical properties, bio-corrosion resistance, and *in vitro* biocompatibility.[6,9,10] Particularly, the $Ti_{47}Cu_{38}Zr_{7.5}Fe_{2.5}Sn_2Si_1Ag_2$ metallic glass showed high GFA, and its critical diameter for glass formation reached 7 mm.[6] The $Ti_{45}Cu_{40}Zr_{7.5}Fe_{2.5}Sn_2Si_1Sc_2$ BMG displayed good plasticity with a large compressive plastic strain approaching 6 pct.[10] Moreover, the Ti-Cu-Zr-Fe-Sn-Si-(Ag, Sc) BMGs exhibited good bio-corrosion resistance, as revealed by their spontaneous passivation behavior and low corrosion rates in the simulated psychological solution.[6,10] Nevertheless, pitting corrosion occurred by the anodic polarization at relatively high potentials in the phosphate buffered saline (PBS) solution for the Ti-Cu-Zr-Fe-Sn-Si-(Ag, Sc) BMGs. Therefore, further improvement of their corrosion resistance is desired.[10–12]

CHENHE WANG, ZHENLONG LIAO, WEI YANG, and TAO ZHANG are with the Key Laboratory of Aerospace Materials and Performance (Ministry of Education), School of Materials Science and Engineering, Beihang University, Beijing 100191, P.R. China. NENGBIN HUA is with the Department of Materials Science and Engineering, Fujian University of Technology, 350118, Fuzhou, P.R. China. SHUJIE PANG is with the Key Laboratory of Aerospace Materials and Performance (Ministry of Education), School of Materials Science and Engineering, Beihang University and also with the Beijing Advanced Innovation Center for Biomedical Engineering, Beihang University, Beijing 100191, P.R. China. Contact e-mail: pangshujie@buaa.edu.cn Peter K. Liaw is with the Department of Materials Science and Engineering, The University of Tennessee, Knoxville, TN 37996.

Manuscript submitted September 22 , 2020; accepted February 1, 2021.

Article published online March 12, 2021

It has been reported that the minor addition of Pd had beneficial effects on improving the corrosion resistance of Ti-based alloys, since Pd is a noble metal element with high chemical stability.[13–15] In addition, it has also been found that the microalloying of Pd in the Zr-based BMGs was favorable for the generation of the icosahedral short/medium-range order, which played an important role in the improvement of GFA and plasticity for the glassy alloys.[13,16] Meanwhile, the addition of Pd in titanium alloys did not show the cytotoxic effect in cell-viability tests.[17,18] Therefore, in the present work, the influences of Pd microalloying on the glass formation, thermal properties, mechanical properties, bio-corrosion behaviors, as well as *in vitro* biocompatibility of the Ti-Cu-Zr-Fe-Sn-Si-Ag glassy alloy were studied, and the biocompatible Ti-Cu-Zr-Fe-Sn-Si-Ag-Pd BMGs with improved mechanical properties and bio-corrosion resistance were developed.

II. MATERIALS AND METHODS

The $Ti_{47}Cu_{38-x}Zr_{7.5}Fe_{2.5}Sn_2Si_1Ag_2Pd_x$ (x = 1, 2, 3, and 4 atomic percent, at. pct) alloy ingots were prepared by arc-melting the mixtures of the pure metals under an Ar atmosphere. The preparation of the cylindrical glassy-alloy rods was carried out by copper-mold casting under a high-purity Ar atmosphere. The microstructure of the specimens was examined, using X-ray diffraction (XRD, Rigaku D/Max2200pc) with the Cu-Kα radiation. The thermal behaviors, including the glass transition, crystallization, and melting of the glassy samples, were characterized by differential scanning calorimetry (DSC, Perkin-Elmer DSC-7 and Netzsch 404C) at a heating rate of 0.33 K/s in a flowing Ar atmosphere.

The uniaxial compressive tests were performed by a SANS CMT5504 materials testing machine at a constant strain rate of 2.1×10^{-4} s^{-1} at room temperature. The stress amplitudes induced by the machine vibration could be no more than 1 MPa. For reproducibility, five glassy rod specimens with the same dimension of ϕ 2×4 mm for each composition were tested. The specimens after deformation were observed by scanning electron microscopy (SEM, JEOL JSM-6010LA). The elastic properties, including the Young's moduli (E) and Poisson's ratios (v), of the glassy samples were determined by an ultrasonic measurement (Olympus Panametrics-NDT 5703PR). Microhardness of the specimens was tested, using a Future-tech FM800 Vickers microhardness tester under a load of 200 g with a dwell time of 12 s. Densities (ρ) of the glassy-alloy rods were measured in the deionized water according to the Archimedean principle.

The bio-corrosion behaviors of the Ti-based BMGs and the Ti-6Al-4V counterpart were characterized by electrochemical experiments with an electrochemical workstation (Princeton Applied Research Versa STAT III) in the Hank's solution (prepared by dissolving 8.00 g/L NaCl, 0.12 g/L $Na_2HPO_4{\cdot}12H_2O$, 0.14 g/L $CaCl_2$, 0.35 g/L $NaHCO_3$, 0.20 g/L $MgSO_4{\cdot}7H_2O$, 0.06 g/L KH_2PO_4, 1.00 g/L $C_6H_{12}O_6$, and 0.40 g/L KCl in the deionized water) at about 310 K, which simulated the physiological environment. The electrochemical tests were carried out in the three-electrode scheme, including the platinum foil counter electrode, the saturated calomel reference electrode (SCE), and the glassy specimens as the working electrode. The preparation procedure of the specimens was the same as that in Ref. [10]. The specimens were immersed in the Hank's solution for about 1200 seconds, and the open-circuit potential (OCP) became almost steady. Subsequently, potentiodynamic polarization was carried out from 50 mV below the OCP of each alloy composition, and then proceeded in the positive direction at a potential scanning rate of 0.833 mV/s. Triplicate specimens were measured to ensure good repeatability for the experiments.

Cell-culture assays were performed for preliminarily assessing the *in vitro* biocompatibility of the Ti-based glassy alloys. The commercial Ti-6Al-4V alloy that has been widely used in the biomedical field was employed for comparison. MC3T3-E1 pre-osteoblasts were cultured in the Dulbecco's modified Eagle's medium (DMEM), which was composed of 10 vol. pct fetal bovine serum (FBS) and 1 vol. pct penicillin (310 K, 5 vol pct CO_2). The alloy specimens were prepared in the same process as that in the previous work.[10] Before the experiments, each side of the specimens was sterilized with the ultraviolet irradiation for 1 hour. After that, the samples were put into a 24-well dish separately while 1 ml cell suspension encompassing of 5×10^3 cells was dripped to the surface of the samples. After cultivating for 24 hours, the cell morphologies on sample surfaces were observed using SEM. The cell viability and potential cytotoxicity were analyzed by the MTT assay [MTT: 3-(4,5-dimethylthiazol-2-yl)-2,5-diphenyl tetrazolium bromide] using an extraction media that have been previously in contact with the samples. After 24 and 72 hours of incubation for cells suspension in the extraction media, respectively, the medium was replaced with a 100 μL MTT solution for further 4-hour incubation. After removing the medium carefully and adding dimethyl sulfoxide (DMSO) in extraction media, the spectrophotometric absorbance was examined at 570 nm on a microplate reader. The trials were performed with three samples for each composition.

III. RESULTS AND DISCUSSION

A. *Formation and Thermal Properties*

Figure 1 shows the XRD patterns of the as-cast $Ti_{47}Cu_{38-x}Zr_{7.5}Fe_{2.5}Sn_2Si_1Ag_2Pd_x$ (x = 1, 2, 3, and 4 at. pct) glassy-alloy rods with their critical diameters (d_c). Each diffraction pattern exhibits a main broad peak and no distinct crystalline peak, indicating that the rod samples are in an amorphous state. It is seen that, for the alloys with Pd contents of 1 and 2 to 4 at. pct, the critical diameters for glass formation are 5 mm and 4 mm, respectively. The results indicate that the present Ti-Cu-Zr-Fe-Sn-Si-Ag-Pd alloys possess high GFA, though the addition of Pd with high contents slightly lowers the critical diameters for glass formation.[6]

Figure 2 displays the DSC curves of the present Ti-based BMGs. As seen in Figure 2(a), the DSC curves

show a glass transition, followed by an endothermic peak corresponding to a supercooled liquid region prior to crystallization. At least two exothermic peaks can be observed on each DSC curve, indicating the multi-stage crystallization behavior of the glassy alloys.[8,19] The values of the d_c, the glass transition temperature (T_g), the onset temperature of crystallization (T_x), the solidus temperature (T_m), the liquidus temperature (T_l), the supercooled liquid region ΔT_x (= T_x − T_g), and the reduced glass transition temperature T_{rg} (= T_g / T_l) are summarized in Table I. It is seen that the glassy alloys exhibit a large supercooled liquid region of 51 to 53 K, which indicates the high thermal stability of the supercooled liquid region against crystallization. In addition, the ΔT_x values of the present Ti-based BMGs are similar to that of the Pd-free $Ti_{47}Cu_{38}Zr_{7.5}Fe_{2.5}Sn_2Si_1Ag_2$ glassy alloy (ΔT_x = 52 K),[6] suggesting that the minor addition of Pd has no distinct effect on the stability of their supercooled liquid.

It is known that the values of T_{rg} (= T_g/T_l) of metallic glasses usually correlate with GFA.[13] Because of the nearly constant viscosity at T_g, the higher ratio of T_g/T_l would result in the higher viscosity at the nose of the Time-Temperature-Transformation (TTT) or Continuous-Cooling-Transformation (CCT) curves, hence leading to the smaller critical cooling rate for glass formation.[13] As seen in Table I, the T_{rg} values of the Pd-bearing Ti-based BMGs are smaller than that of the $Ti_{47}Cu_{38}Zr_{7.5}Fe_{2.5}Sn_2Si_1Ag_2$ BMG, which is corresponding to the results mentioned above that the Pd alloying with high contents slightly lowers the GFA of the Ti-based BMGs.[6]

B. *Mechanical Properties*

Figure 3 shows the stress–strain curves of the Ti-Cu-Zr-Fe-Sn-Si-Ag-Pd BMGs under compression. The compressive yield strength (σ_y), fracture strength (σ_f), and plastic strain (ε_p) of the Ti-based BMGs are summarized in Table II. The present BMGs exhibit yield strengths above 2000 MPa, followed by the plastic deformation with a strain of ~ 2.5 to 4.5 pct. The result indicates that the addition of Pd is favorable for improving the plasticity of the resultant Ti-Cu-Zr-Fe-Sn-Si-Ag-Pd BMGs.[6] The morphologies of the fractured Ti-Cu-Zr-Fe-Sn-Si-Ag-Pd BMGs are displayed in Figures 4(a) through (d). It can be observed that the fracture occurred along the main shear plane that declined by about 43 deg to the direction of the compression load. The lateral surfaces of the fractured samples show abundant primary shear bands parallel to the principal shear front, while the secondary shear bands distribute in irregular directions. Moreover, it can be seen that typical vein patterns exist on the fracture

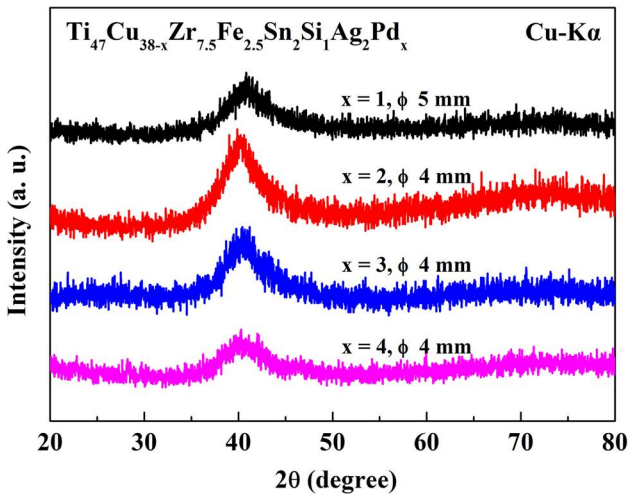

Fig. 1—XRD patterns of the $Ti_{47}Cu_{38-x}Zr_{7.5}Fe_{2.5}Sn_2Si_1Ag_2Pd_x$ (x = 1, 2, 3, and 4 at. pct) BMGs with their critical diameters.

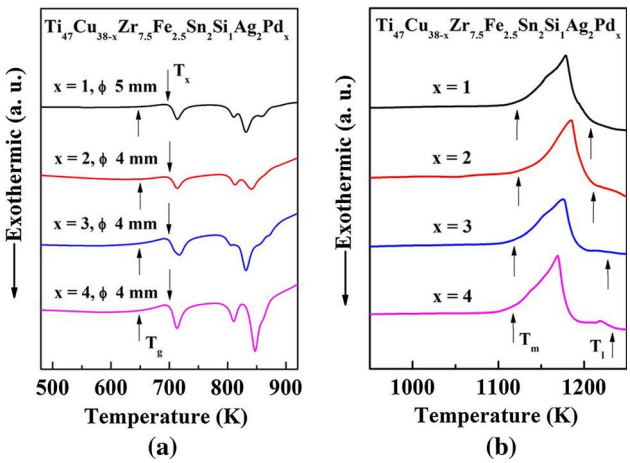

Fig. 2—DSC curves of the $Ti_{47}Cu_{38-x}Zr_{7.5}Fe_{2.5}Sn_2Si_1Ag_2Pd_x$ (x = 1, 2, 3, and 4 at. pct) BMGs with their critical diameters: (*a*) crystallization and (*b*) melting behaviors.

Table I. Thermal Properties and d_c for Glass Formation of the $Ti_{47}Cu_{38-x}Zr_{7.5}Fe_{2.5}Sn_2Si_1Ag_2Pd_x$ (x = 0, 1, 2, 3, and 4 at. pct) BMGs

Alloys	T_g (K)	T_x (K)	ΔT_x (K)	T_m (K)	T_l (K)	T_g/T_l	d_c (mm)
x = 0 [6]	641	693	52	1116	1180	0.543	7
x = 1	648	699	51	1122	1206	0.537	5
x = 2	650	701	51	1125	1211	0.536	4
x = 3	649	700	51	1121	1228	0.529	4
x = 4	648	701	53	1118	1232	0.526	4

surface. These characteristics of the deformation and fracture are typical of the BMGs with good plasticity.[8]

It is notable that the $Ti_{47}Cu_{38-x}Zr_{7.5}Fe_{2.5}Sn_2Si_1Ag_2Pd_x$ (x = 2 and 3 at. pct) glassy alloys possess the significant plastic strain of around 4 pct. For a better understanding of their plasticity, Figure 5 shows the enlargement of the partial plastic-deformation regions on the stress–strain curves of the $Ti_{47}Cu_{38-x}Zr_{7.5}Fe_{2.5}Sn_2Si_1Ag_2Pd_x$ (x = 1, 2, 3, and 4 at. pct) BMGs displayed in Figure 3. It can be observed that the large serrations are followed by a series of small serrations, corresponding to the generation of secondary shear bands after the release of the primary shear band during the plastic deformation of the Ti-based BMGs.[20] It can also be seen that the amplitudes of the large serration events for the $Ti_{47}Cu_{38-x}Zr_{7.5}Fe_{2.5}Sn_2Si_1Ag_2Pd_x$ (x = 2 and 3 at. pct) alloys are generally smaller than those of the BMGs with 1 and 4 at. pct Pd. In the process of the plastic deformation, the smaller amplitudes of stress drops in serrated flows represent the shorter sliding distance and higher shear-band stability of the glassy alloys,[20,21] resulting in the good plasticity of the BMGs containing 2 and 3 at. pct Pd.

Moreover, it is known that the plastic deformation of BMGs is associated with the free volume.[22] It has been proved that a large amount of randomly distributing free volumes play a dominant role in improving the plasticity of BMGs.[22] The content of free volumes presented in the BMGs is strongly linked to the area of the exothermic peak prior to T_g of the DSC curves.[23] Figure 6 shows the enlargement of the DSC curves of the $Ti_{47}Cu_{38-x}Zr_{7.5}Fe_{2.5}Sn_2Si_1Ag_2Pd_x$ (x = 1, 2, 3, and 4 at. pct) BMGs near T_g. It can be seen that the areas of the exothermic peak before T_g of the $Ti_{47}Cu_{38-x}Zr_{7.5}Fe_{2.5}Sn_2Si_1Ag_2Pd_x$ (x = 2 and 3 at. pct) BMGs are larger than those of the 1 and 4 at. pct Pd-alloying BMGs, which indicates that more free volumes are involved in the BMGs containing 2 and 3 at. pct Pd. During the compression process, the free volumes facilitate the movement of the atoms near the crack tip to accelerate the stress relaxation and even allow small cracks to be healed by themselves, which expands the displacement of the critical shear before fracture.[22] In addition, a large amount of free volumes with a random distribution in different regions of the specimens could promote the shear-band nucleation, propagation, and intersection to hinder the primary shearing process, and facilitate the good plasticity.[24] Therefore, the 2 and 3 at. pct Pd-alloying BMGs with more free volumes could possess better plasticity.

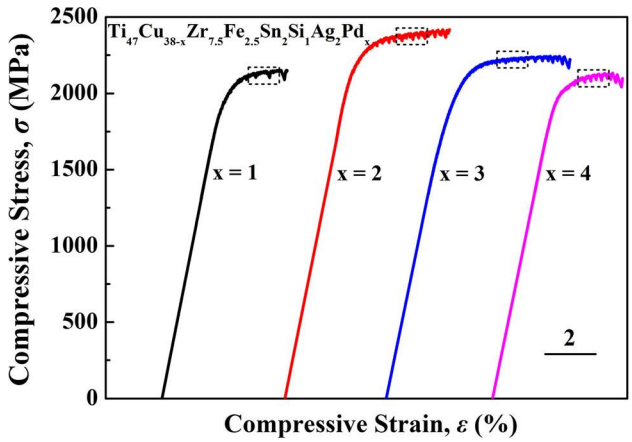

Fig. 3—Compressive stress–strain curves of the $Ti_{47}Cu_{38-x}Zr_{7.5}Fe_{2.5}Sn_2Si_1Ag_2Pd_x$ (x = 1, 2, 3, and 4 at. pct) BMGs.

It is also worth noting that, as shown in Table II, the $Ti_{47}Cu_{38-x}Zr_{7.5}Fe_{2.5}Sn_2Si_1Ag_2Pd_x$ (x = 2 and 3 at. pct) BMGs have relatively high Poisson's ratios in the present Ti-based BMGs, which may provoke the increase in the shear-transformation-zone (STZ) volumes during the deformation process of glassy-alloy rods.[25] The large-sized STZs can prevent the shear softening and facilitate the generation of multiple branched shear bands during plastic flows,[26,27] as observed on the lateral surface of $Ti_{47}Cu_{38-x}Zr_{7.5}Fe_{2.5}Sn_2Si_1Ag_2Pd_x$ (x = 2 and 3 at. pct) alloy rods (Figures 4(b) and (c)), which is consistent with their relatively large compressive plastic strain.

The Young's modulus (E), specific strength (σ_y/ρ), Vickers microhardness (H_v), the ratio of microhardness to the Young's modulus (H_v/E), and Poisson's ratio (v) of the present Ti-based BMGs are also presented in Table II. It can be seen that the Young's moduli of the present Ti-based BMGs (~ 100 GPa) are less than that of the Ti-6Al-4V alloy (~ 110 to 125 GPa).[28,29] The relatively lower Young's moduli contribute to alleviating the "stress-shielding effect," which is necessary for implant materials to match with the hard tissue in the service process.[30] Furthermore, the Ti-based BMGs

Table II. Mechanical Properties of the $Ti_{47}Cu_{38-x}Zr_{7.5}Fe_{2.5}Sn_2Si_1Ag_2Pd_x$ (x = 0, 1, 2, 3, and 4 at. pct) BMGs

Alloys	ρ (g/cm^3)	σ_y (MPa)	ε_p (Pct)	σ_f (MPa)	σ_y/ρ ($\times 10^5$ N m/kg)	H_v	E (GPa)	H_v/E	v
x = 0 [6]	6.238	2028 ± 32	2.5 ± 0.2	2081 ± 18	3.2 ± 0.1	588 ± 6	100.4 ± 0.2	0.059	0.359 ± 0.001
x = 1	6.367 ± 0.008	2019 ± 34	2.5 ± 0.2	2183 ± 23	3.2 ± 0.1	594 ± 8	100.5 ± 0.3	0.059 ± 0.001	0.359 ± 0.001
x = 2	6.408 ± 0.006	2098 ± 43	3.7 ± 0.3	2340 ± 56	3.3 ± 0.1	610 ± 7	100.6 ± 0.2	0.061 ± 0.001	0.360 ± 0.001
x = 3	6.453 ± 0.003	2035 ± 30	4.5 ± 0.3	2241 ± 32	3.2 ± 0.1	596 ± 9	100.9 ± 0.2	0.059 ± 0.001	0.360 ± 0.001
x = 4	6.515 ± 0.005	2017 ± 53	3.0 ± 0.2	2174 ± 54	3.1 ± 0.1	591 ± 6	101.3 ± 0.3	0.059 ± 0.001	0.360 ± 0.001

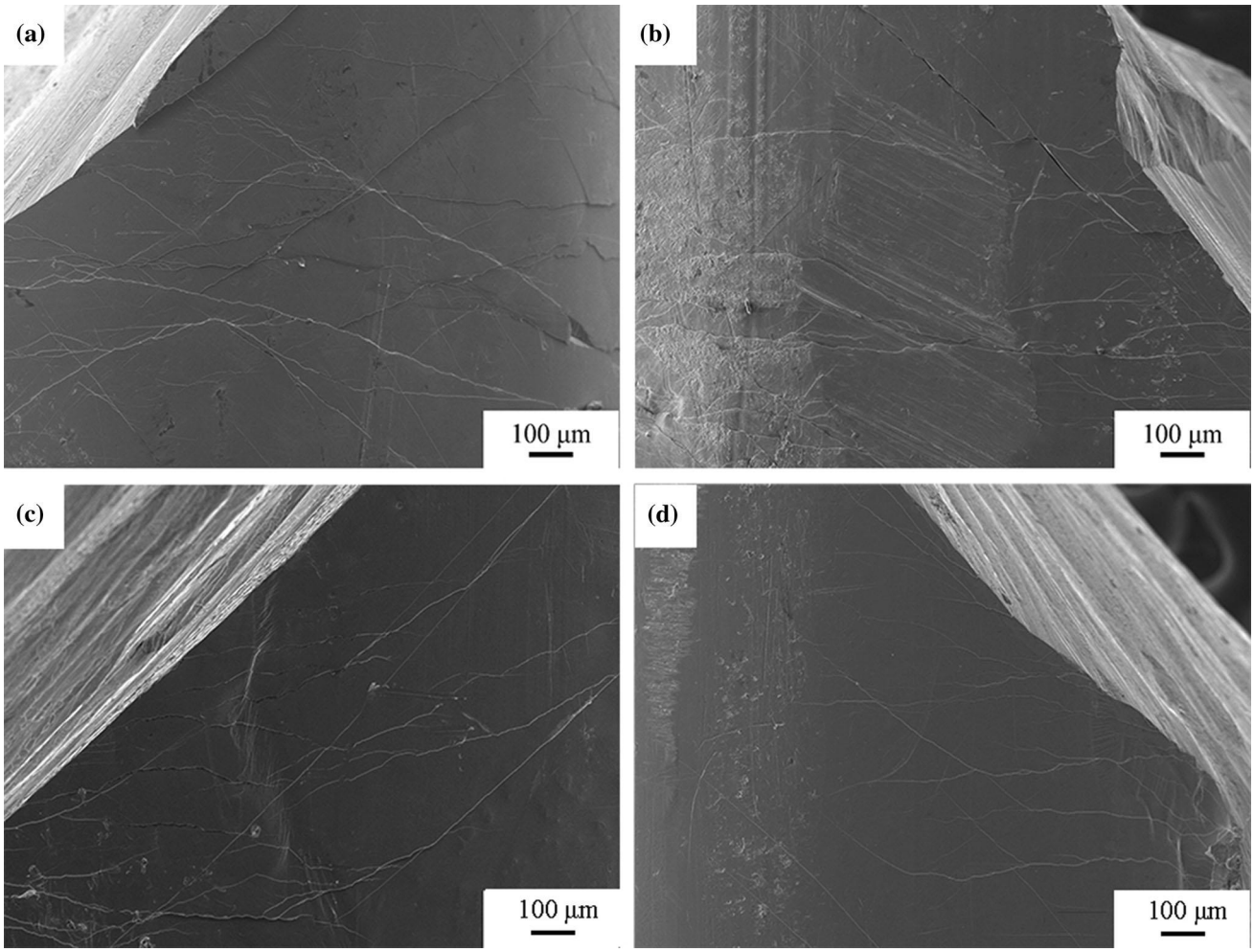

Fig. 4—The morphologies of the fractured $Ti_{47}Cu_{38-x}Zr_{7.5}Fe_{2.5}Sn_2Si_1Ag_2Pd_x$ BMGs: (*a*) $x = 1$, (*b*) $x = 2$, (*c*) $x = 3$, and (*d*) $x = 4$.

present Vickers microhardness of 591 to 610 Hv, and H_v/E of about 0.059 to 0.061, which are higher than those of the Ti-6Al-4V alloy ($H_v = \sim 320$ Hv and $H_v/E = \sim 0.026$ to 0.029), suggesting that the present metallic glasses may possess better wear resistance.[29] The high strength and microhardness, relatively low Young's modulus, and good plasticity suggest that the Pd-microalloying Ti-based BMGs have the potential to be used as biomaterials.

C. *Bio-corrosion Behaviors*

After the 30-day immersion in the Hank's solution at 310 K, the present Ti-Cu-Zr-Fe-Sn-Si-Ag-Pd BMGs exhibit no detectable mass loss and no obvious change in surface morphologies, indicating their high bio-corrosion resistance. The bio-corrosion behaviors of the Ti-based metallic glasses were further investigated by electrochemical measurements in the Hank's solution at 310 K. The immersion-time dependence of the OCPs and the polarization curves of the Ti-based BMGs and the Ti-6Al-4V alloy are presented in Figure 7(a). It is seen that the potentials of the alloys initially rise abruptly, and then increase slowly until reach stationary values. After the 1200 seconds immersion, there are no significant differences in the OCPs of the $Ti_{47}Cu_{38-x}Zr_{7.5}Fe_{2.5}Sn_2Si_1Ag_2Pd_x$ ($x = 0$, 1, 2, 3, and 4 at. pct) BMGs. Compared with that of the Ti-6Al-4V alloy, the OCPs of the Ti-based BMGs are higher, suggesting that the surfaces of the metallic glasses have higher stability. The polarization curves of the Ti-based BMGs presented in Figure 7(b) are characterized by the spontaneous passivation with a wide passive region and low passive current density, though pitting corrosion occurs at high anodic potentials. It is well known that the pitting corrosion behavior of a BMG is closely related to its chemical composition.[31,32] In the surface film of the Ti-Cu-Zr-Fe-Sn-Si-Ag system BMGs, zirconium could exist in the form of ZrO_2,[10] which is sensitive to the chloride ions in the Hank's solution. The reaction of the ZrO_2 and Cl^- leads to the breakdown of passive films on the surfaces of the Ti-based BMGs, which results in the pitting corrosion of the material eventually.[33] Besides, Cu and Sn are more likely to react with chloride ions to form $CuCl^{2-}$ and $SnCl^+$ complexes in a neutral solution, inducing the instability and thinning of the surface film and further leading to the pitting corrosion of the present Ti-based BMGs.[31] This trend is also consistent

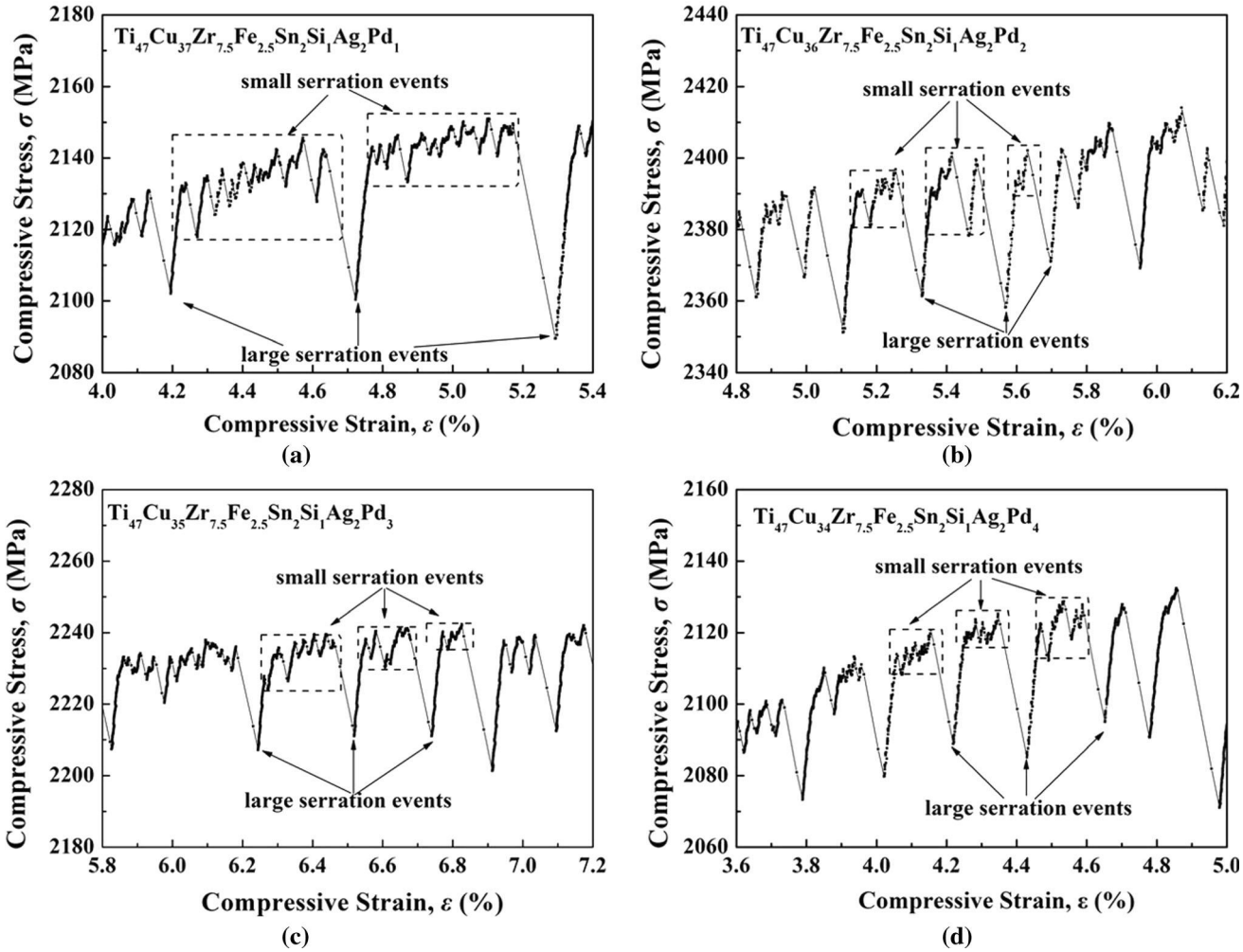

Fig. 5—The enlargement of the partial plastic-deformation region on the stress–strain curves of the $Ti_{47}Cu_{38-x}Zr_{7.5}Fe_{2.5}Sn_2Si_1Ag_2Pd_x$ BMGs displayed in Fig. 3: (*a*) $x = 1$, (*b*) $x = 2$, (*c*) $x = 3$, and (*d*) $x = 4$.

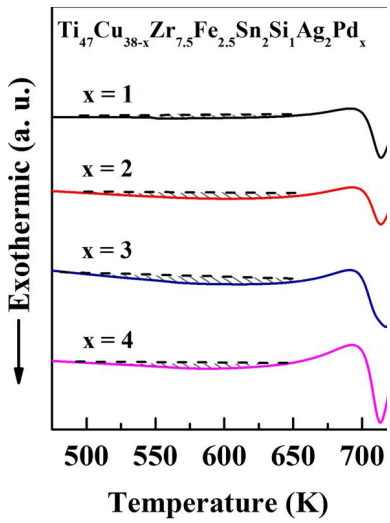

Fig. 6—The enlargement of the DSC curves near the T_g for the $Ti_{47}Cu_{38-x}Zr_{7.5}Fe_{2.5}Sn_2Si_1Ag_2Pd_x$ ($x = 1$, 2, 3, and 4 at. pct) BMGs.

with the result that the pitting resistance is improved through substituting Cu with the addition of 2 to 4 at. pct Pd for the present Ti-based BMGs. In addition, it is notable that the Pd-bearing Ti-based BMGs exhibit lower passive current densities than that of the Pd-free Ti-based BMG and the Ti-6Al-4V alloy. The values of the corrosion potential (E_{corr}), the pitting potential (E_{pit}), the passivation region ($E_{pass} = E_{pit} - E_{corr}$), the corrosion current density (i_{corr}), and the corrosion rate calculated from the i_{corr} are summarized in Table III. The corrosion rates of the Ti-Cu-Zr-Fe-Sn-Si-Ag-Pd glassy alloys are within the scope from 5.6×10^{-4} to 7.4×10^{-4} mm/year, which are comparable with that of the Ti-6Al-4V alloy and lower than that of the Pd-free Ti-based BMG. These results suggest the good bio-corrosion resistance of the Ti-Cu-Zr-Fe-Sn-Si-Ag-Pd BMGs in the simulated human body environment.

For the Ti-based glassy alloys with amorphous structures, the homogeneous single solid-solution phase nature can eliminate heterogeneities,[3,4,34] which contributes to the formation of a uniform passive layer on the alloy surface in the Hank's solution. Due to the passivity of Pd as a noble metal element, the

microalloying of Pd could enhance the protectiveness of the passive films on the alloys, which prevents the ion transport and reduces the dissolution rate of the passive layer.[34] Thus, the microalloying of Pd in the Ti-based BMGs facilitates the good bio-corrosion resistance in the simulated physiological environment.

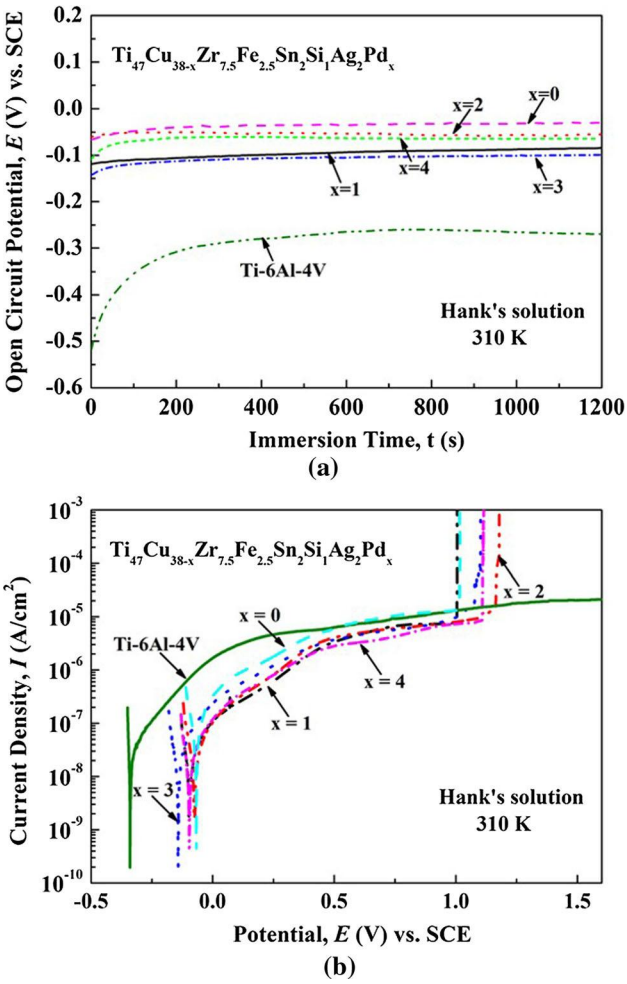

Fig. 7—(*a*) Changes in the OCPs with the immersion time and (*b*) potentiodynamic polarization curves of the $Ti_{47}Cu_{38-x}Zr_{7.5}Fe_{2.5}Sn_2Si_1Ag_2Pd_x$ (x = 0, 1, 2, 3, and 4 at. pct) BMGs and the Ti-6Al-4V alloy in the Hank's solution at 310 K.

D. *In Vitro Biocompatibility*

In vitro cell responses of the $Ti_{47}Cu_{36}Zr_{7.5}Fe_{2.5}Sn_2Si_1Ag_2Pd_2$ BMG were investigated by cell-culture experiments to preliminarily assess the biocompatibility of the Pd-bearing Ti-based glassy alloys as potential biomedical implants. The commercial Ti-6Al-4V alloy and the Pd-free Ti-based BMG were utilized as references. Similar cellular behaviors on the surfaces of the Ti-based BMGs and Ti-6Al-4V alloy, including the normal cell adhesion behavior and the morphologies of cells, are revealed in the cell-culture assays. Figure 8 provides the MC3T3-E1 cell morphologies after cultivating for 24 hours on the surfaces of the $Ti_{47}Cu_{38-x}Zr_{7.5}Fe_{2.5}Sn_2Si_1Ag_2Pd_x$ (x = 0 and 2 at. pct) BMGs and Ti-6Al-4V alloy. As illustrated in Figures 8(a), (c), and (e), it is seen that the cells are well spread and extended, and a certain number of interacted cells attach on the alloy surfaces. Figures 8(b), (d), and (f) show the magnified SEM images of the corresponding detailed cell morphologies on the three specimens. All the adherent cells on the surface of each substrate present similar irregular, polygonal, and spindle-like shapes after 24-hour culturing, which is an indication that the cell adhesion and growth of the cells were healthy.[35]

The MTT assay results of the cell viability and proliferation for the $Ti_{47}Cu_{38-x}Zr_{7.5}Fe_{2.5}Sn_2Si_2Ag_2Pd_x$ (x = 0 and 2 at. pct) metallic glasses and the Ti-6Al-4V alloy are illustrated in Figure 9. In all sample extracts, the optical density (O. D.) values of MC3T3-E1 cells significantly increase from the culturing of 24 to 72 hours. The results represent that more viable cells are present in the media over time, indicating the normal cell proliferation.[5] Besides, the O. D. values of the $Ti_{47}Cu_{36}Zr_{7.5}Fe_{2.5}Sn_2Si_1Ag_2Pd_2$ alloy are comparable to that of the Pd-free alloy, indicating that microalloying of the Pd into the Ti-based BMGs shows insignificant influence on the cell proliferation. Furthermore, there is no significant difference in O. D. values of MC3T3-E1 cells among the three alloys at each time point, suggesting that cell viabilities of the $Ti_{47}Cu_{38-x}Zr_{7.5}Fe_{2.5}Sn_2Si_1Ag_2Pd_x$ (x = 0 and 2 at. pct) BMGs groups are comparable to that of the Ti-6Al-4V alloy. Therefore, it is concluded that microalloying of Pd is favorable for the cell growth and proliferation on the Ti-based BMGs. The experiment results demonstrate that the Pd-bearing Ti-based BMGs have good *in vitro* biocompatibility.

Table III. Values of the Electrochemical Parameters Derived from the Potentiodynamic Polarization Curves for the $Ti_{47}Cu_{38-x}Zr_{7.5}Fe_{2.5}Sn_2Si_1Ag_2Pd_x$ (x = 0, 1, 2, 3, and 4 at. pct) BMGs and the Ti-6Al-4V Alloy in the Hank's Solution at 310 K

Alloys	E_{corr} (V) *vs* SCE	i_{corr} ($\times 10^{-7}$ A/cm^2)	E_{pit} (V) *vs* SCE	$E_{pit} - E_{corr}$ (V) *vs* SCE	Corrosion Rate ($\times 10^{-4}$ mm/year)
x = 0	− 0.08 ± 0.05	1.82 ± 0.06	1.02 ± 0.08	1.1 ± 0.07	17.4 ± 0.4
x = 1	− 0.12 ± 0.03	0.63 ± 0.08	1.01 ± 0.07	1.13 ± 0.09	5.9 ± 0.7
x = 2	− 0.11 ± 0.04	0.79 ± 0.06	1.18 ± 0.09	1.29 ± 0.11	7.4 ± 0.3
x = 3	− 0.13 ± 0.07	0.69 ± 0.05	1.11 ± 0.06	1.24 ± 0.07	6.4 ± 0.5
x = 4	− 0.06 ± 0.04	0.58 ± 0.07	1.12 ± 0.07	1.18 ± 0.08	5.6 ± 0.3
Ti-6Al-4V	− 0.3 ± 0.04	0.62 ± 0.08	—	—	5.6 ± 0.4

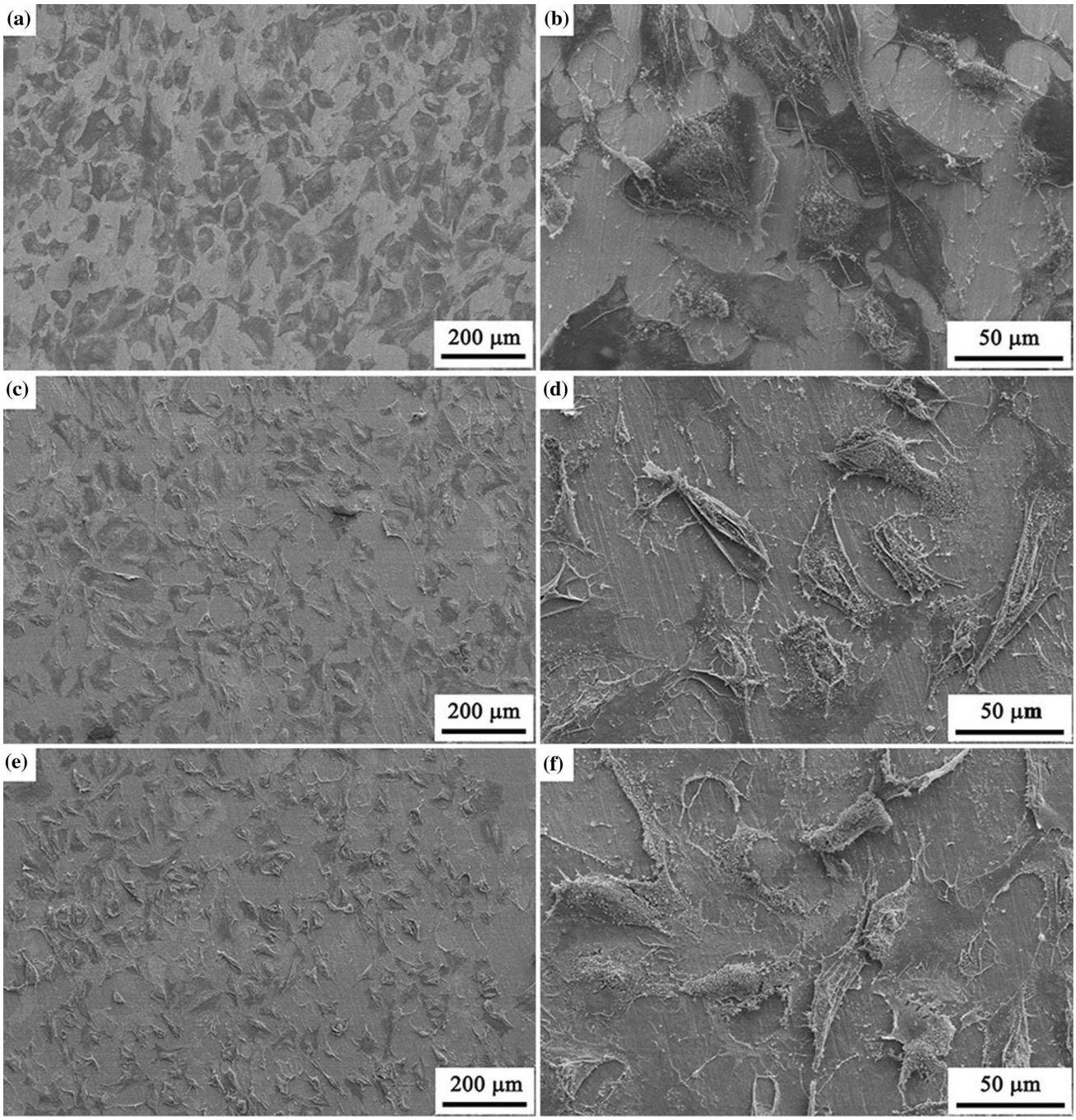

Fig. 8—Morphologies of MC3T3-E1 cells cultured on (*a*) and (*b*) the $Ti_{47}Cu_{38}Zr_{7.5}Fe_{2.5}Sn_2Si_1Ag_2$ BMG, (*c*) and (*d*) the $Ti_{47}Cu_{36}Zr_{7.5}Fe_{2.5}Sn_2Si_1Ag_2Pd_2$ BMG, and (*e*) and (*f*) the Ti-6Al-4V alloy for 24 h.

IV. CONCLUSIONS

The Ti-based $Ti_{47}Cu_{38-x}Zr_{7.5}Fe_{2.5}Sn_2Si_1Ag_2Pd_x$ (x = 1, 2, 3, and 4 at. pct) BMGs free from highly toxic elements are developed, and their critical diameters for glass formation by a copper-mold casting are 4 to 5 mm, and the intervals of the supercooled liquid region are up to 51 to 53 K. The present Ti-based BMGs exhibit relatively low Young's moduli of about 100 GPa, high strengths of over 2000 MPa, and high microhardness of 591 to 610 Hv. Particularly, the $Ti_{47}Cu_{38-x}Zr_{7.5}Fe_{2.5}Sn_2Si_1Ag_2Pd_x$ (x = 2 and 3 at. pct) BMGs possess good plasticity with compressive plastic strains of around 4 pct. Furthermore, the addition of Pd results in the decrease in the passive current density and the increase in the pitting potential of the Ti-based BMGs in the Hank's solution, leading to their good bio-corrosion resistance. The normal MC3T3-E1 cell adhesions and proliferations demonstrate the good *in vitro* biocompatibility of the Ti-Cu-Zr-Fe-Sn-Si-Ag-Pd BMGs parallel to that of the Ti-6Al-4V alloy. The Ti-Cu-Zr-Fe-Sn-Si-Ag-Pd BMGs with the improved mechanical

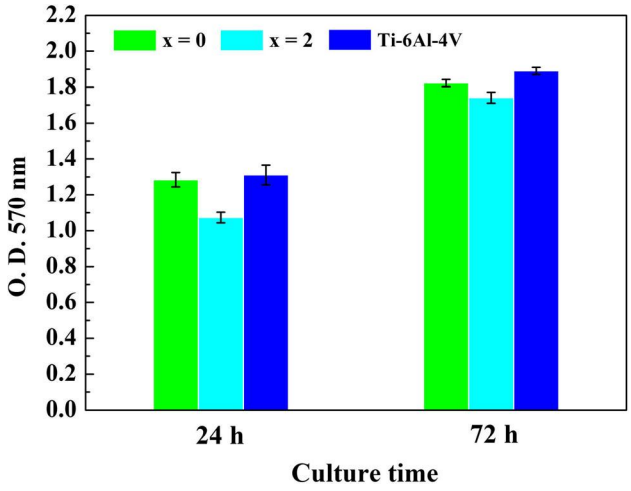

Fig. 9—Proliferation of MC3T3-E1 cells cultured in the extraction media from the $Ti_{47}Cu_{38-x}Zr_{7.5}Fe_{2.5}Sn_2Si_1Ag_2Pd_x$ (x = 0 and 2 at. pct) BMGs and the Ti-6Al-4V alloy for 24 and 72 h, respectively.

properties, good bio-corrosion resistance, and *in vitro* biocompatibility are promising to be potential biomedical materials.

ACKNOWLEDGMENTS

The authors are grateful to the financial support by the National Natural Science Foundation of China (No. 51671008). P. K. L. very much appreciates the supports from the National Science Foundation [DMR-1611180 and 1809640] with the program directors, Drs. Judith Yang, Gary Shiflet, and Diana Farkas.

REFERENCES

1. H.F. Li and Y.F. Zheng: *Acta Biomater.*, 2016, vol. 36, pp. 1–20.
2. M.D. Demetriou, A. Wiest, D.C. Hofmann, W.L. Johnson, B. Han, N. Wolfson, G.Y. Wang, and P.K. Liaw: *JOM*, 2010, vol. 62, pp. 83–91.
3. J. Schroers, G. Kumar, M. Thomas, S.C. Hodges, and R.T. Kyriakides: *JOM*, 2009, vol. 61, pp. 21–29.
4. G.Q. Xie, F.X. Qin, and S.L. Zhu: *Mater. Trans.*, 2013, vol. 54, pp. 1314–23.
5. T.H. Li, P.C. Wong, S.F. Chang, P.H. Tsai, J.S.C. Jang, and J.C. Huang: *Mater. Sci. Eng. C*, 2017, vol. 75, pp. 1–6.
6. S.J. Pang, Y. Liu, H.F. Li, L.L. Sun, Y. Li, and T. Zhang: *J. Alloys Compd.*, 2015, vol. 625, pp. 323–27.
7. A. Kuball, O. Gross, B. Bochtler, B. Adam, L. Ruschel, M. Zamanzade, and R. Busch: *J. Alloys Compd.*, 2019, vol. 790, pp. 337–46.
8. S.L. Zhu, X.M. Wang, F.X. Qin, and A. Inoue: *Mater. Sci. Eng. A*, 2007, vol. 459, pp. 233–37.
9. Y. Liu, S.J. Pang, H.F. Li, Q. Hu, B. Chen, and T. Zhang: *Intermetallics*, 2016, vol. 72, pp. 36–43.
10. Y. Liu, G. Wang, H.F. Li, S.J. Pang, K.W. Chen, and T. Zhang: *J. Alloys Compd.*, 2016, vol. 679, pp. 341–49.
11. T. Hanawa: *Sci. Tech. Adv. Mater.*, 2002, vol. 3, pp. 289–95.
12. U.K. Mudali, S. Baunack, J. Eckert, L. Schultz, and A. Gebert: *J. Alloys Compd.*, 2004, vol. 377, pp. 290–97.
13. W.H. Wang: *Prog. Mater. Sci.*, 2007, vol. 52, pp. 540–96.
14. C.T. Liu and Z.P. Lu: *Intermetallics*, 2005, vol. 13, pp. 415–18.
15. C. Leyens and M. Peters: *Titanium and Titanium Alloys. Fundamentals and Applications*, WILEY-VCH, Germany, 2003, pp. 17–20.
16. J. Saida, A.D. Setyawan, H. Kato, M. Matsushita, and A. Inoue: *Mater. Trans.*, 2008, vol. 49, pp. 2732–36.
17. J.C. Hornez, A. Lefèvre, D. Joly, and H.F. Hildebrand: *Biomol. Eng.*, 2002, vol. 19, pp. 103–17.
18. Y. Okazaki and E. Gotoh: *Biomaterials*, 2005, vol. 26, pp. 11–21.
19. A. Inoue, N. Nishiyama, K. Amiya, T. Zhang, and T. Masumoto: *Mater. Lett.*, 1994, vol. 19, pp. 131–35.
20. G.N. Yang, S.Q. Chen, J.L. Gu, S.F. Zhao, J.F. Li, Y. Shao, H. Wang, and K.F. Yao: *Philos. Mag.*, 2016, vol. 96, pp. 2243–55.
21. L. Zhang, F. Jiang, Y. Zhao, and S.B. Pan: *J. Mater. Res.*, 2010, vol. 25, pp. 283–91.
22. P. Murali and U. Ramamurty: *Acta Mater.*, 2005, vol. 53, pp. 1467–78.
23. A. Slipenyuk and J. Eckert: *Scr. Mater.*, 2004, vol. 50, pp. 39–44.
24. L.Y. Chen, A.D. Setyawan, H. Kato, A. Inoue, G.Q. Zhang, J. Saida, X.D. Wang, Q.P. Cao, and J.Z. Jiang: *Scripta Mater.*, 2008, vol. 59, pp. 75–78.
25. D. Pan, A. Inoue, T. Sakurai, and M.W. Chen: *PNAS*, 2008, vol. 105, pp. 14769–72.
26. R. Tao and Z.F. Zhang: *Sci. Rep.*, 2013, vol. 3, pp. 1–6.
27. G. Pan, D. Lei, J.S. Jin, S.B. Wang, X.Y. Wang, and K.F. Yao: *Metals*, 2016, vol. 37, pp. 1–37.
28. M.L. Morrison, R.A. Buchanan, R.V. Leon, C.T. Liu, B.A. Green, P.K. Liaw, and J.A. Horton: *J. Biomed. Mater. Res. Part A*, 2005, vol. 74, pp. 430–38.
29. P. Gong, K.F. Yao, and Y. Shao: *J. Alloy. Compd.*, 2012, vol. 536, pp. 26–29.
30. A. Leyladn and A. Matthews: *Wear*, 2000, vol. 246, pp. 1–11.
31. A. Liens, B. Ter-Ovanessian, N. Courtois, D. Fabregue, and J. Chevalier: *Corros. Sci.*, 2020, vol. 177, p. 108854.
32. J.L. Gu, S.Y. Lu, Y. Shao, and K.F. Yao: *Corros. Sci.*, 2020, vol. 178, p. 109078.
33. L. Huang, Y. Yokoyama, W. Wu, P.K. Liaw, S.J. Pang, A. Inoue, T. Zhang, and W. He: *J. Biomed. Mater. Res. B*, 2012, vol. 100B, pp. 1472–82.
34. J.L. Gu, X.L. Yang, A.L. Zhang, Y. Shao, S.F. Zhao, and K.F. Yao: *J. Non-Cryst. Solids*, 2019, vol. 512, pp. 206–10.
35. Y. Guo, I. Bataev, K. Georgarakis, A.M. Jorge, Jr, R.P. Nogueira, M. Pons, and A.R. Yavari: *Intermetallics*, 2015, vol. 63, pp. 86–96.